Desalination and Water Treatment
www.deswater.com

doi: 10.1080/19443994.2014.903523

54 (2015) 2856–2867
May

Taylor & Francis
Taylor & Francis Group

Functionalization of polyacrylonitrile nanofiber mat via surface-initiated atom transfer radical polymerization for copper ions removal from aqueous solution

Jianqiang Wang, Peng Jia, Kai Pan*, Bing Cao*

Key Laboratory of Carbon Fiber and Functional Polymers, Ministry of Education, Beijing University of Chemical Technology, Beijing 100029, China, Tel. +86 10 64413857; Fax: +86 10 64436876; email: pankai@mail.buct.edu.cn (K. Pan); bcao@mail.buct.edu.cn (B. Cao)

Received 18 September 2013; Accepted 7 March 2014

ABSTRACT

Poly (acrylic acid) (PAAc)-functionalized PAN nanofiber (PAN-COOH) mats were prepared via electrospinning followed by atom transfer radical polymerization for the removal of copper ions from aqueous solution. Attenuated total reflections Fourier transform infrared and X-ray photoelectron spectroscopy results confirmed the presence of PAAc layer on the surface of PAN nanofibers. The morphology of PAN-COOH nanofibers was studied by scanning electron microscopy. Adsorption results indicated that the adsorption capacity was pH dependent. Adsorption equilibrium reached within 30 min as the initial solution concentration increased from 108 to 268 mg/L, and the process can be described using the pseudo-second-order model. Isotherm data fitted well to the Langmuir isotherm model. Desorption results showed that adsorption capacity can remain up to 90% after five times usage.

Keywords: Nanofiber; ATRP; Adsorption; Heavy metal ion

1. Introduction

Recently, the concern for heavy metal ions contamination due to chemical and industrial processes has been increased. Copper ion is one of the most common toxic heavy metal ions. Accumulation of Cu^{2+} will be toxic [1]. The World Health Organization recommends the maximum allowable limit of copper in the drinking water is 2.0 mg/L [2]. Therefore, Cu^{2+} should be removed from aqueous solution, in order to avoid the deleterious impact of Cu^{2+} on human health.

Several technologies have been developed for the removal of Cu^{2+} from aqueous solution, such as electrodeposition [3,4], ion exchange [5,6], membrane separation [7–11], adsorption [12–16], etc. Compared to other methods, adsorption is simple and effective due to its easiness to operate and simplicity to design. Several kinds of materials were used as adsorbent for heavy metal ions, such as active carbon, metal oxide nanoparticles, agricultural waste, etc. However, these kinds of absorbents suffer from a common problem that it needs a later separation process from the solution, which will increase the operation cost. For avoiding this problem, some researchers use polymer fiber membrane as the adsorbent. For example, Deng et al. [17] used aminated polyacrylonitrile (PAN) fibers (diameters were in the range of about 20–50 μm) for the adsorption of Cu^{2+} ions from aqueous solution

---

*Corresponding author.

and the aminated PAN fibers exhibit high adsorption capacity.

Recently, polymer nanofibers obtained by electrospinning were used as adsorbent for its small diameter and easy preparation. This kind of adsorbent has a high surface area because of the nanoscale diameter of the polymer nanofibers; moreover, functional groups on the surface of nanofibers can be changed by using different polymer or modification. Chitosan nanofiber mat obtained by electrospinning was used for the adsorption of Cu^{2+} ions after chemical neutralization of ammonium into amine group [18]. Polyethyleneimine nanofibers, with a large amount of amino and imino groups in its polymer chain, were obtained by electrospinning directly, and used for the adsorption of Cu^{2+} ions [19,20]. Electrospun PAN nanofiber mats were most commonly used in the adsorption of heavy metal ions for its easy preparation and modification. Aminated electrospun PAN nanofiber mat was used as adsorbent for heavy metal ions [21–23]. Amino groups are highly active in the formation of strong complexes with metal ions because they contain nitrogen atoms. Meanwhile, adsorbents modified by carboxylic groups (which contain oxygen atoms) such as chitosan-g-poly (acrylic acid) attapulgite composites, carboxylic acid-functionalized konjac glucomannan, and chitosan/poly (acrylic acid) (PAAc) magnetic composite microspheres exhibit high adsorption capacity for Cu^{2+} ions [24–27].

Therefore, in this study, carboxylic groups were introduced onto the surface of PAN nanofibers by the method of atom transfer radical polymerization (ATRP). Firstly, PAN nanofiber mat was obtained by electrospinning. Secondly, polydopamine was deposited on the surface of PAN nanofibers. Finally, PAAc was grafted after the immobilization of ATRP initiator. And then the functionalized PAN nanofiber mats were used for adsorption of Cu^{2+} ions from aqueous solutions.

2. Experimental setup

2.1. Chemicals

PAN ($M_n = 150{,}000$), $CuCl_2{\cdot}2H_2O$, copper (I) chloride (CuCl), HPLC water, and 2,2-dipyridyl (bpy) were purchased from Sigma-Aldrich (Steinheim, Germany) and used as received. 2-bromoisobutyryl bromide (2-BIB 97%), dopamine hydrochloride (99%), and tris (hydroxymethyl) aminomethane (99%) were purchased from Alfa Aesar and used as received. *N*, *N*-dimethylformamide (DMF), acrylic acid (AAc), tetrahydrofuran (THF), and triethylamine were purchased from Sinopharm Chemical Reagent Co., Ltd AAc, THF and triethylamine were distillated before use.

2.2. Electrospinning of PAN nanofiber mat

The electrospinning process for PAN nanofiber mat has been reported in our previously published papers [28,29].

2.3. Immobilization of ATRP initiators on PAN nanofiber surface

The PAN nanofiber mat was first heat treated at 140℃ for 2 h to improve the integration and then washed with ethanol. After dried for a certain time in the vacuum oven, the immobilization of ATRP initiators onto the surface of PAN nanofiber mat was carried out. Firstly, heat-treated PAN nanofiber mats were immersed into dopamine solution (dopamine was dissolved in 10 mM Tris-HCl with a concentration of 2 g/L, pH 8.5) and shaken for 2 h in a thermostatic shaker at 27℃ to introduce hydroxyl groups. Secondly, hydroxyl groups on the surface of PAN-OH nanofibers reacted with 2-BIB to obtain 2-bromoisobutyryl bromide-immobilized PAN-Br nanofiber mat. For the reaction, 35 mL of THF and 3 mL of triethylamine were introduced into a bottle containing PAN-OH nanofiber mat, followed by the addition of 0.5 mL of 2-BIB. The mixed reaction solution was shaken in a thermostatic shaker bath, operating at 25℃ under argon atmosphere for 3 h. Finally, the PAN-Br nanofiber mat was rinsed by THF and dried in the vacuum oven.

2.4. Surface-initiated ATRP on PAN nanofibers

HPLC water, copper (I) chloride, 2,2-bipyridyl, NaOH, NaCl, AAc, and PAN-Br nanofiber mat were added into three-mouth flask. Before the polymerization reaction, the flask was backfilled with nitrogen for 15 min. The reaction mixture was shaken for 30 min at 27℃, during which the flask was de-oxygenated by inletting nitrogen. After polymerization, the mats functionalized by PAAc were washed in water for three times under stirring, the first at room temperature, the second at 45℃, and the third at room temperature too, and then PAN-COOH nanofiber mats were dried in vacuum drying oven.

2.5. Cu^{2+} ions adsorption experiments

Copper sulfate was used as the source of Cu^{2+}. 100 mg dry PAN-COOH nanofiber mats were added into 20 mL 170 mg/L Cu^{2+} solutions with different pH for 12 h. The pH of the Cu^{2+} solution was adjusted by HCl solution. The removal percentage of Cu^{2+} can be calculated by Eq. (1):

$$\% \text{ Removal} = \frac{C_0 - C_e}{C_0} \times 100 \tag{1}$$

where C_0 is the initial concentration of Cu^{2+} in solution (mg/L) and C_e is the equilibrium concentration (mg/L).

The adsorption isotherms for Cu^{2+} were established by batch adsorption experiments. 100 mg PAN-COOH nanofiber mats were immersed into 20 mL Cu^{2+} solutions with different concentration. The initial pH of the Cu^{2+} solutions was adjusted to 5.0 by NaOH solution. The adsorption was carried out at 25℃ with constant shaking, and then kept for 12 h to establish adsorption equilibrium. The equilibrium adsorption capacity was determined using Eq. (2):

$$q_e = \frac{C_0 - C_e}{m} V \tag{2}$$

where C_0 is the initial concentration of Cu^{2+} in solution (mg/L), C_e is the equilibrium concentration (mg/L), q_e is the equilibrium adsorption capacity (mg/g), m is the mass of adsorbents (g), and V is the volume of solution (L).

The kinetic adsorption performance was studied by contacting 100 mg of PAN-COOH nanofiber mat with Cu^{2+} solutions of different initial concentration at 25℃. The initial pH of the Cu^{2+} solution is 5.0, and the solution was shaken during this process. Samples were taken out of the solution at different time, each time 0.1 mL. The adsorption capacity was calculated by Eq. (3):

$$q_t = \frac{C_0 - C_t}{m} V \tag{3}$$

where q_t (mg/g) is the adsorption capacity at time t, C_0 is the initial concentration of Cu^{2+} in solution (mg/L), C_t is the Cu^{2+} concentration at time t (mg/L), m is the mass of adsorbent (g), and V is the volume of solution (L).

2.6. Desorption experiment

For desorption studies, 100 mg PAN-COOH nanofiber mats were first contacted with 20 mL 170 mg/L Cu^{2+} for 12 h at 25℃. Then, the adsorbent was immersed into 20 mL 0.2 M HCl solution for 10 min at 25℃. The above procedure was repeated for five times to test the reusability of the adsorbent.

2.7. Apparatus and instrumentation

The functional groups on the surface of samples were detected by attenuated total reflections Fourier transform infrared (ATR-FTIR) spectrometer using a Perkin-Elmer spectrum RXI. The resolution is 4 cm^{-1}. The surface chemical compositions of pristine PAN nanofibers and the modified nanofibers were analyzed by X-ray photoelectron spectroscopy (XPS) using Thermo Electron Corporation ESCALAB250 equipment with an Al Kα X-ray source (1486.6 eV).The surface morphologies of the nanofiber mat were studied by Hitachi S-4700 scanning electron microscopy (SEM). Cu^{2+} concentration was measured with an inductively coupled plasma mass spectrometry (7700 series, Agilent technologies).

3. Results and discussion

3.1. Surface chemical compositions study of the nanofiber mat

To anchor the ATRP initiator 2-BIB onto the nanofiber surface, PAN nanofiber mat was first coated by polydopamine using a procedure similar to that described in the literature [30]. The polydopamine-coated PAN nanofibers can offer catechol groups which can be used to anchor the ATRP initator 2-BIB [31]. The modification process is shown in Fig. 1. Fig. 2 shows the ATR-FTIR results of PAN-Br, PAN-COOH with different AAc concentration, and PAN-COOH treated by acid solution (pH 2.0). It is observed that after AAc polymerization on the surface of PAN nanofibers, the absorption bands assigned to carboxylate, and hydroxyl groups appeared at 1,571 and 3,353 cm^{-1}, respectively [26]. Fig. 2(d) shows a wide and broad peak at about 3,353 cm^{-1}, which may be due to self-polymerization of AAc at high AAc concentration. During AAc polymerization process, pH of the AAc solution was adjusted to about 10 by adding NaOH and NaCl. Therefore, carbonyl appeared as the style of carboxylate. However, an obvious hypsochromic shift can be observed (from 1,571 to 1,718 cm^{-1}) after immersed into acid solution (pH 2.0) for 30 min. The hypsochromic shift is due to the transform from carboxylate to carboxylic acid [32].

XPS was also used to study the chemical composite of PAN nanofiber mat before and after modification. Br3d and Br3p were clearly observed after 2-BIB anchored onto the surface of PAN nanofibers as shown in Fig. 3(a). The bromine content on the surface of

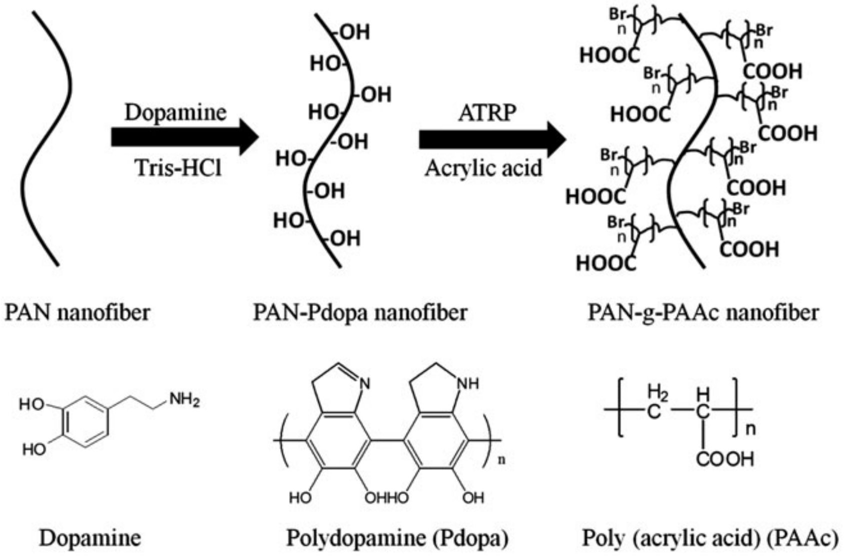

Fig. 1. Schematic illustration of the ATRP of AAc on polydopamine-functionalized PAN nanofiber.

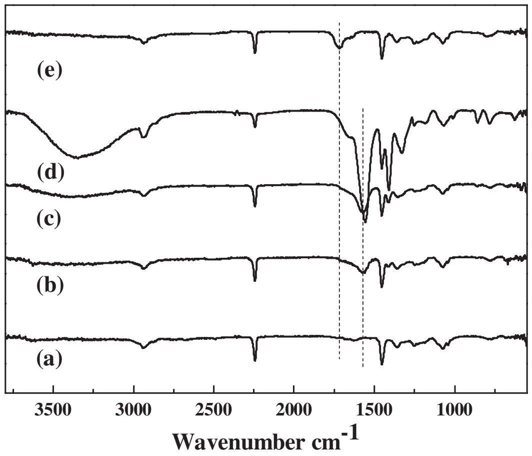

Fig. 2. ATR-FTIR spectra of (a) PAN-Br, (b) PAN-COOH 9% AAc, (c) PAN-COOH 12% AAc, (d) PAN-COOH 15% AAc, and (e) PAN-COOH 12% AAc, treated by acid solution.

PAN-Br nanofiber mat was 0.77 atom%. The oxygen content increased from 8.77 to 25.64 atom% after AAc polymerization onto the surface of PAN-Br nanofiber mat. Meanwhile, the oxygen content increased with AAc monomer concentration increased (as shown in Table 1). The nitrogen content decreased from 10.65 to 2.46 atom% for the absence of nitrogen atom in the PAAc chain. Since AAc was transferred to acrylate before ATRP, 4.42–7.57 atom% of natrium was detected after modification using different monomer concentration. It is worth mentioning that the natrium content decreased from 6.57 to 0.36 atom% after immersed into the acid solution (pH 2.0), another evidence for the conversion of carboxylate to carboxylic acid groups. The results indicate that PAAc was successfully grafted onto the surface of the PAN nanofibers.

3.2. *Morphology of the nanofiber mats*

The morphology of the nanofiber mat was studied by SEM, and the results were shown in Fig. 4. Some of the PAN nanofibers were connected together after polydopamine coated on the surface of PAN nanofibers (as shown in Fig. 4(b)). Initiator immobilization process nearly did not affect the nanofiber morphology (as shown in Fig. 4(c)). However, after modification by ATRP with AAc, nanofibers were connected together obviously for the PAAc chains grafted onto the surface of PAN nanofibers. The spacing between the nanofibers was almost covered by PAAc, while the AAc concentration was 15%. However, when the AAc concentration was below 12%, pores between nanofibers were retained and still in the macro-meter scale. Therefore, PAN-COOH obtained by 12% AAc was used in the following adsorption experiments for enough carboxylic acid groups and high surface area.

3.3. *pH effect on the adsorption*

Adsorbents functionalized by weak acid are much dependent on the pH value of solution. When the adsorbents are non-ionized at low pH, they are poor interaction with heavy metal ions. However, adsorption–desorption process can be easily realized by

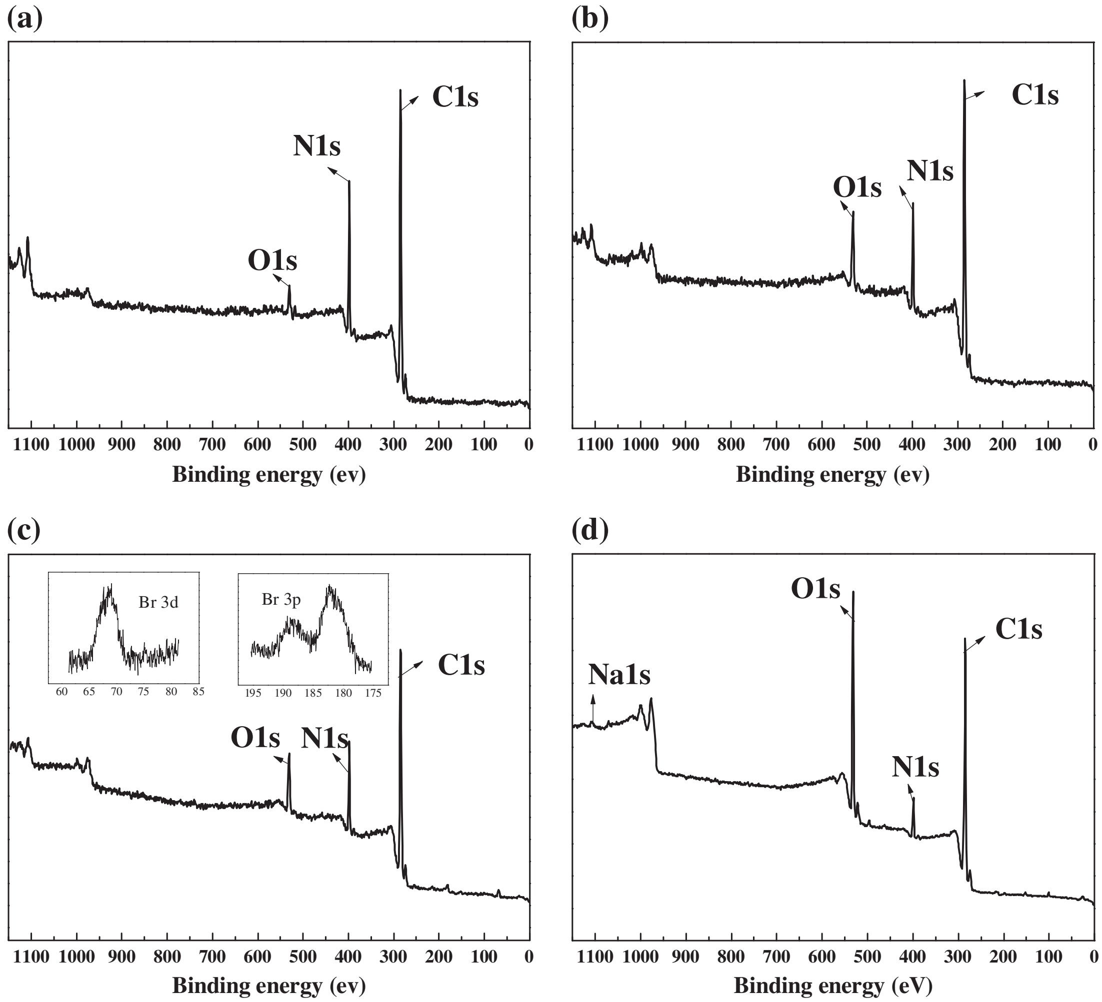

Fig. 3. XPS wide scan spectra of (a) PAN nanofibers, (b) PAN nanofibers coated by polydopamine, (c) PAN-Br nanofibers, and (d) PAN-COOH of 12% AAc.

Table 1
XPS results of nanofiber mat

	C1s (atom %)	O1s (atom %)	N1s (atom %)	Br3d (atom %)	Na1s (atom %)
PAN	76.81	3.96	19.24		
PAN-dopa 2 h	78.4	7.83	13.77		
PAN-Br	79.8	8.77	10.65	0.77	
PAN-COOH 9% AAc	71.21	14.59	9.57	0.21	4.42
PAN-COOH 12% AAc	68.49	18.04	6.58	0.32	6.57
PAN-COOH 15% AAc	64.33	25.64	2.46		7.57
PAN-COOH 12% AAc (treated by acid solution)	71.64	22.15	5.85		0.36

adjusting the pH of the solution [33]. The adsorption of metal ions on the surface of PAN-COOH nanofiber mat was studied and the results are shown as a function of initial pH of the solution in Fig. 5. When the pH of the solution was higher than 6.0, precipitation of Cu^{2+} ions as $Cu(OH)_2$ would occur spontaneously [34]. Therefore, the measured pH range was from 2.0 to 5.0. When the pH of the initial solution changed from 2.0 to 5.0, the adsorption efficiency increased from 4.77 to nearly 90%. In our previous work, we found that when pH value was 3.6, the carboxyl group of PAAc existed in the form of undissociated acid, and the hydrogen bond was strong, so the chain of PAAc shrank. With the pH value increasing, hydrogen bond became weak, and the grafted chains stretched [35]. Therefore, the reason for the low adsorption efficiency at low pH is due to the

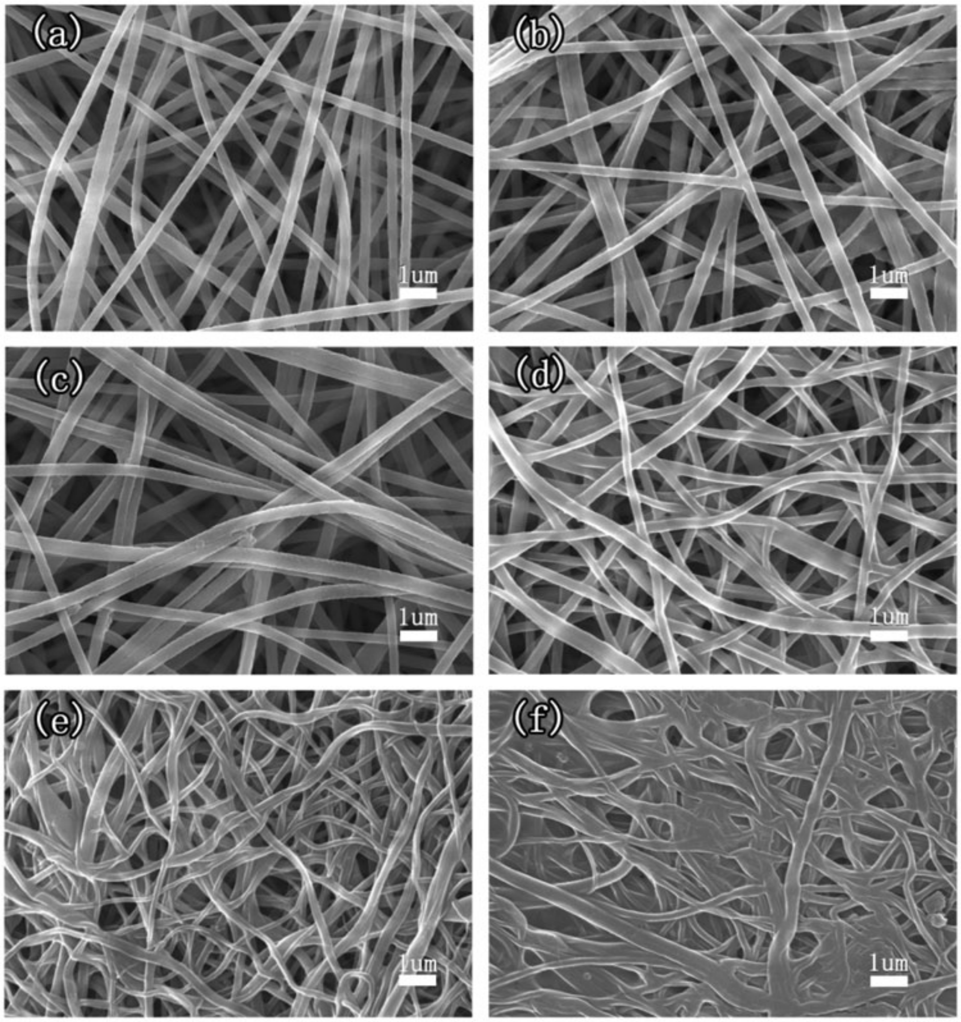

Fig. 4. SEM images of nanofiber mat, (a) pure PAN; (b) PAN-Pdopa 2 h; (c) PAN-Br; (d) PAN-COOH, 9% AAc; (e) PAN-COOH, 12% AAc; (f) PAN-COOH, 15% AAc.

undissociated carboxyl groups and competitive interaction between H^+ ions and Cu^{2+} ions for the same sorption sites on adsorbent surface. However, carboxyl groups in polymer chains dissociated and stretched at higher pH, and the adsorption efficiency increases due to the interaction of static electricity. The following adsorption isotherms and kinetic properties were performed at the condition of initial pH 5.0 of the solution.

3.4. Effect of adsorbent dose

The dosage of adsorbent used in the adsorption process is an important factor, which determines the capacity of the adsorbent for a given initial concentration. To study the dosage effect on Cu^{2+} ions removal performance, different amount of PAN-COOH nanofiber mats was added into 20 mL 170 ppm Cu^{2+}

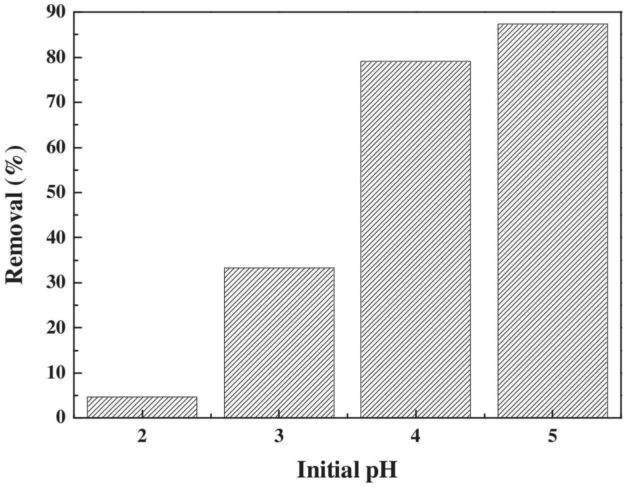

Fig. 5. Effect of pH on the adsorption of Cu^{2+} ions.

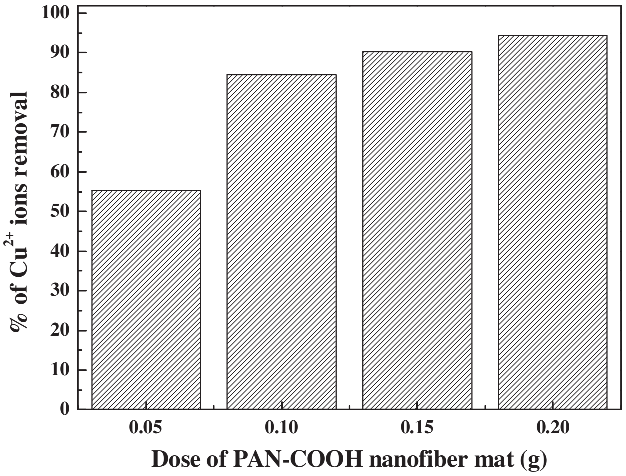

Fig. 6. Effect of PAN-COOH nanofiber mat dose on Cu^{2+} ions removal performance.

ions solution (pH 5.0) for 12 h. The results were shown in Fig. 6. The results indicated that the percentage removal of Cu^{2+} ions rapidly increased (from 55.2 to 94.3%) with the increase of mat dosage (from 0.05 to 0.20 g). The increase of removal performance for Cu^{2+} ions is due to the more available sorption sites. However, when the dosage of PAN-COOH nanofiber mats was more than 0.1 g, the percentage removal of Cu^{2+} ions slightly increased.

3.5. Adsorption kinetics

The effect of adsorption time on adsorption capacity at different initial solution concentration is shown in Fig. 7. The results indicate that the adsorption capacity of Cu^{2+} ions increases with an increase in adsorption time until equilibrium is reached between adsorbents and Cu^{2+} ions. The equilibrium time was about 30 min and almost unchanged as the initial solution concentration increased from 108 to 268 mg/L. The equilibrium capacity is 16.71, 35.07, and 48.20 mg/g for 108, 182, and 268 mg/L initial Cu^{2+} ions solution, respectively.

In order to better understand the adsorption behaviors, adsorption kinetic data are often analyzed using two commonly used kinetic models, namely the pseudo-first-order [36] and the pseudo-second-order [37] kinetic model. These two kinetic models are used to describe the adsorption of solid/liquid systems, which can be expressed in the linear forms as Eqs. (4) and (5), respectively:

$$\log(q_e - q_t) = \log q_e - \frac{K_1}{2.303}t \tag{4}$$

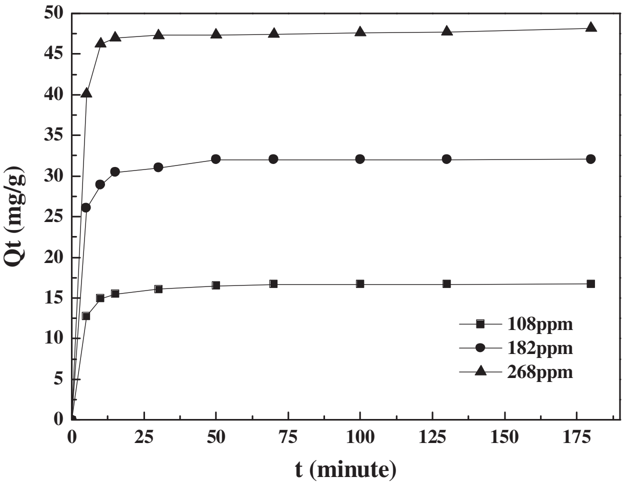

Fig. 7. Effect of contact time and initial concentration on the adsorption of Cu^{2+} ions onto PAN-COOH nanofiber mats.

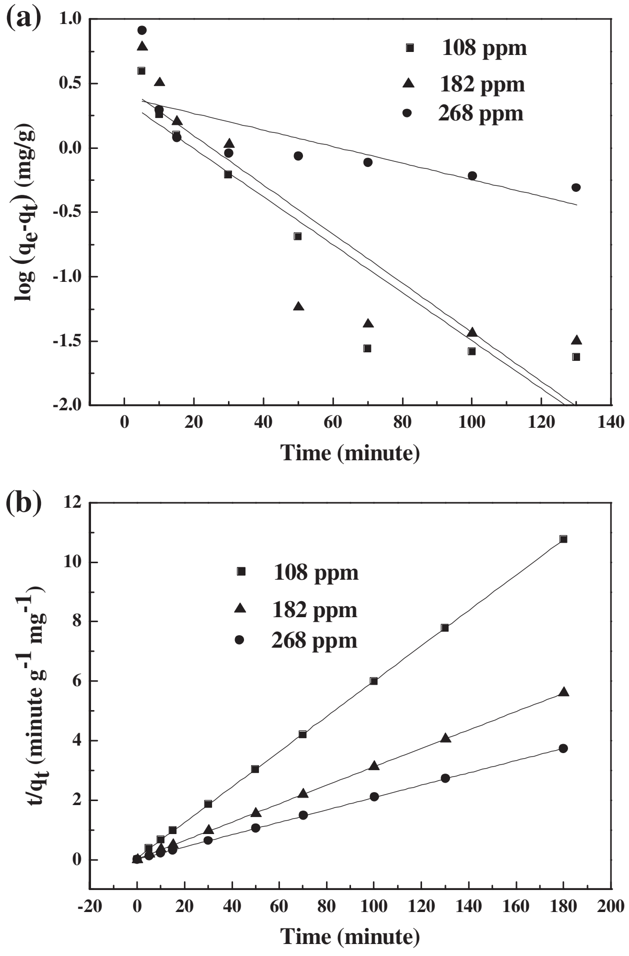

Fig. 8. Pseudo-first-order kinetic model (a), pseudo-second-order kinetic model (b) for adsorption of Cu^{2+} ions on PAN-COOH nanofiber mats.

Table 2
Kinetics parameters for Cu^{2+} ions adsorption onto PAN-COOH nanofiber mat

		Pseudo-first-order model			Pseudo-second-order model		
C_0 (mg/L)	$q_{e,exp}$ (mg/g)	K_1 (1/min)	$q_{e,cal}$ (mg/g)	R^2	K_2 (g/mg/min)	$q_{e,cal}$ (mg/g)	R^2
108	16.71	0.043	2.32	0.85614	0.059	16.82	0.99994
182	35.07	0.044	1.11	0.76776	0.041	32.23	0.99995
268	48.20	0.015	2.48	0.50223	0.033	48.15	0.99993

Notes: $q_{e,exp}$: equilibrium adsorption capacity from experiments; $q_{e,cal}$: equilibrium adsorption capacity calculated from the kinetic models.

$$\frac{t}{q_t} = \frac{1}{K_2 q_e^2} + \frac{1}{q_e} t \tag{5}$$

where K_1 and K_2 are the pseudo-first-order and second-order rate constants, respectively.

The adsorption kinetic plots for the adsorption of Cu^{2+} ions are shown in Fig. 8, and the obtained kinetic parameters are summarized in Table 2. The values of the correlation coefficients (shown in Table 2) clearly indicated that the adsorption kinetics closely followed the pseudo-second-order model rather than the pseudo-first-order model. The pseudo-second-order rate constant (K_2) decreased from 0.059 to 0.033 g/mg/min with an increase in initial concentration from 108 to 268 mg/L. Moreover, $q_{e,cal}$ values obtained from pseudo-second-order kinetic model appeared to be very close to the experimentally observed values than values from pseudo-first-order kinetic model.

3.6. Adsorption isotherm

Adsorption isotherms were investigated to exhibit the adsorption capacity of PAN-COOH nanofiber mat for Cu^{2+} ions removal. The adsorption isotherms of Cu^{2+} ions removal by PAN-COOH nanofiber mat are shown in Fig. 9. It can be observed that there is an increase of q_e with an increase of C_e, and q_e increases faster at lower C_e than at high C_e.

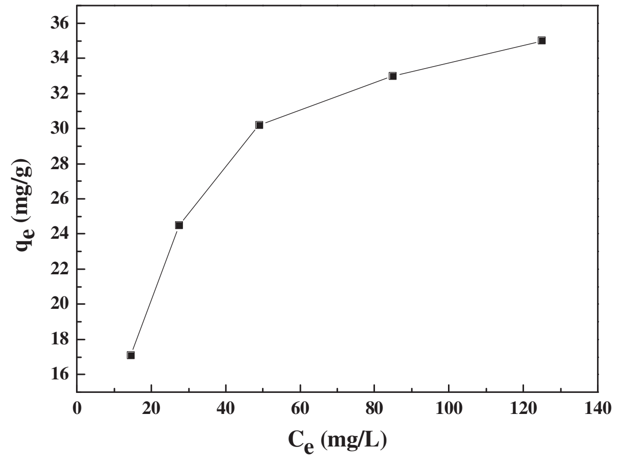

Fig. 9. Equilibrium isotherms of Cu^{2+} ions adsorption onto PAN-COOH nanofiber mat.

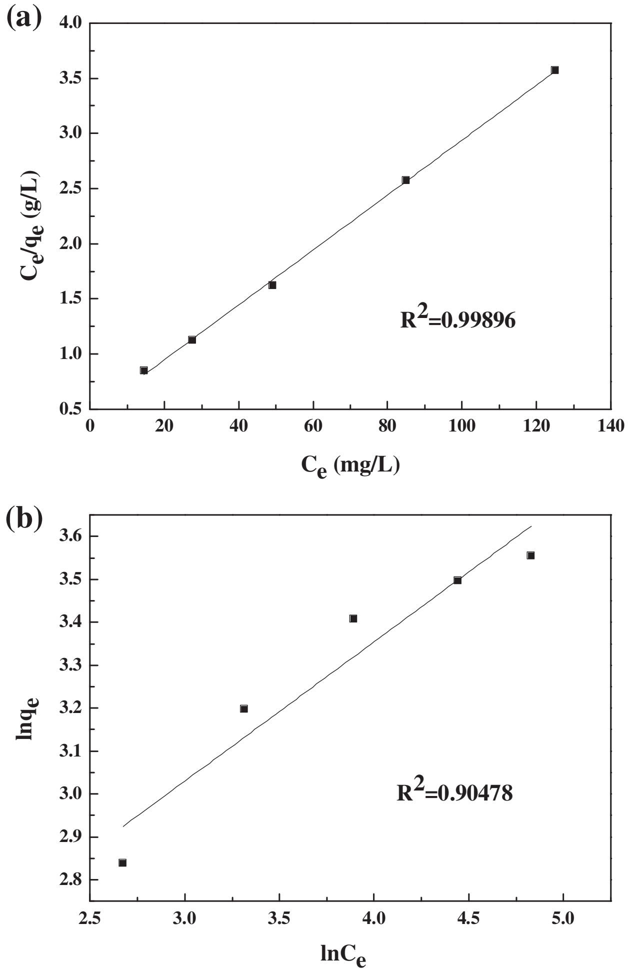

Fig. 10. Langmuir isotherm model (a) and Freundlich isotherm model (b) for adsorption of Cu^{2+} ions onto PAN-COOH nanofiber mat.

Table 3
Langmuir and Freundlich isotherm parameters for Cr(VI) adsorption onto PAN/PANI nanofiber mat

Langmuir model			Freundlich model		
q_m (mg/g)	b (L/mg)	R^2	K_f (mg/g)	$1/n$	R^2
40.145	0.056	0.99896	7.812	0.325	0.90478

Two well-known models [38] of Langmuir and Freundlich isotherms were used to fit the equilibrium data, and the correlation coefficient (R^2) obtained was used to evaluate the fit of the two models. The Langmuir model is based on the assumption of adsorption homogeneity, representing equally available adsorption sites, monolayer surface coverage, and no interaction between adsorbed species. The linearized Langmuir isotherm model is represented by Eq. (6):

$$\frac{C_e}{q_e} = \frac{1}{q_m b} + \frac{C_e}{q_m} \tag{6}$$

The Freundlich isotherm describes reversible adsorption and is not restricted to the formation of the monolayer. This empirical equation takes the form, as shown in Eq. (7):

$$\ln q_e = \ln K_f + \frac{\ln C_e}{n} \tag{7}$$

where q_m (mg/g) is the maximum adsorption capacity, b (L/mg) is the Langmuir constant related to the energy of adsorption, and K_f and $1/n$ constants are related to the adsorption capacity and intensity of adsorption, respectively.

The fitted plots for the two models are shown in Fig. 10, and the obtained kinetic parameters are summarized in Table 3. The higher values of correlation coefficient indicated that Langmuir model better fitted the isotherm data than Freundlich model. The maximum adsorption capacity calculated from Langmuir model is up to 40.14 mg/g.

Table 4 summarized the adsorption performance for Cu^{2+} ions of different adsorbents reported by other literatures. It was observed that amine-functionalized adsorbents present high adsorption capacity for Cu^{2+} ions. However, this kind of adsorbents needs a long time (usually several hours) to reach the adsorption equilibrium [17–21,23]. Although the adsorption capacity of carboxylic acid-functionalized adsorbents was a little lower than amine groups-functionalized adsorbents, the adsorption rate was much fast. Commonly, adsorption equilibrium will be reached within one hour [24–26]. Therefore, PAN-COOH nanofiber adsorbents not only avoid the later separation process, but also have a much fast adsorption rate.

3.7. Adsorption mechanism

To further study the adsorption process, PAN-COOH nanofiber mat before and after Cu^{2+} ions was examined by ATR-FTIR, and the results were shown in Fig. 11. It can be observed that two strong peaks appeared at about 1,711 and 1,449 cm^{-1} in both PAN-COOH nanofiber before and after Cu^{2+} ions, which ascribed to asymmetric and symmetric stretching of C=O in PAAc, respectively [39]. However, two new peaks appeared at about 1,613 and 1,413 cm^{-1} after Cu^{2+} ions adsorption, which may be due to the formation of metal–ligand bond between Cu^{2+} ions and carboxyl oxygen [40–42]. Since the coordination number of Cu^{2+} ion is 4 [43], a plausible mechanism for the

Table 4
Comparison of adsorption performance of the PAN/PANI mat with other adsorbents for Cr(VI)

	Type	q_m (mg/g)	Equilibrium time (h)	Optimum pH	Refs.
With amine or imine groups	Fiber mat	31.45	About 3 for 132 mg/L Cu^{2+}	4.5	[17]
With amine or imine groups	Nanofiber mat	485.44	About 4 for 400 mg/L Cu^{2+}	No result	[18]
With amine or imine groups	Nanofiber mat	70.92	About 6 for 100 mg/L Cu^{2+}	5.0	[19]
With amine or imine groups	Nanofiber mat	161.29	About 5	5–7	[20]
With amine or imine groups	Nanofiber mat	150.60	About 10 for 200 mg/L Cu^{2+}	4.0	[21]
With amine or imine groups	Nanofiber mat	116.52	About 0.33 for 590 mg/L Cu^{2+}	5–6	[22]
With amine or imine groups	Nanofiber mat	31.30	About 5 for 200 mg/L Cu^{2+}	5	[23]
With carboxylic acid groups	Powder	303	About 1 for 1,220 mg/L Cu^{2+}	5.5	[24]
With carboxylic acid groups	Powder	64.5	About 0.33 for 1,000 mg/L Cu^{2+}	5.0	[25]
With carboxylic acid groups	Powder	177	About 0.58 for 385 mg/L Cu^{2+}	5.5	[26]

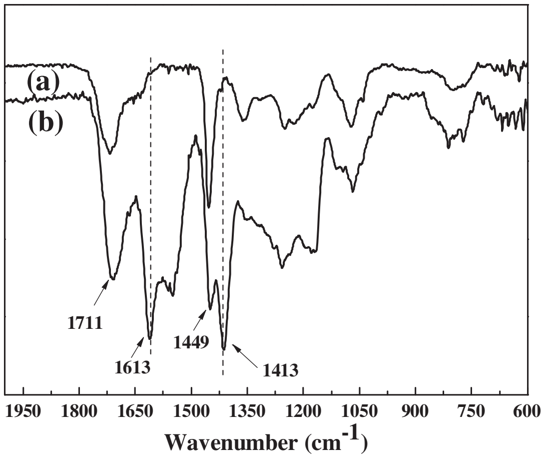

Fig. 11. ATR-FTIR study of PAN-COOH nanofiber mat before (a) and after (b) Cu^{2+} ions adsorption.

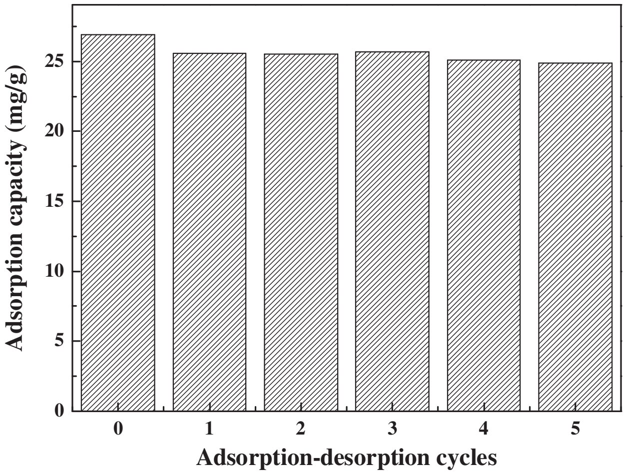

Fig. 13. Adsorption–desorption cycles.

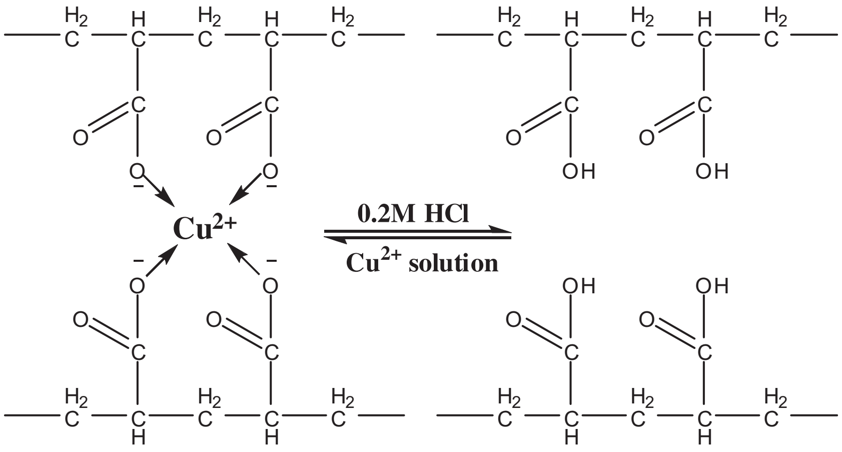

Fig. 12. A plausible mechanism for the adsorption and desorption of Cu^{2+} ions.

adsorption and desorption of Cu^{2+} ions was proposed as shown in Fig. 12.

3.8. Desorption performance of the PAN-COOH nanofiber mat

Since the adsorption of Cu^{2+} ions onto PAN-COOH nanofiber mat is pH dependent and lower pH is beneficial for Cu^{2+} ions adsorption, the desorption of Cu^{2+} ions from adsorbents can be achieved by decreasing system pH values. Therefore, for the reuse ability study, 0.2 M HCl was used to regenerate the PAN-COOH nanofiber mat loaded with Cu^{2+} ions. As shown in Fig. 13, the adsorption capacity was still kept more than 90% of the original adsorption capacity after five times usage. The results indicate the potential application of PAN-COOH nanofiber mats in wastewater treatment.

4. Conclusions

PAN-COOH nanofiber mats were successfully prepared by electrospinning method followed by ATRP. And then the PAN-COOH nanofiber mats were used as adsorbent for Cu^{2+} ions from aqueous solution. ATR-FTIR and XPS results show that PAAc layer was coated on the surface of PAN nanofibers. The PAAc layer can be clearly seen from the SEM images. The adsorption capacity was pH dependent. The removal percentage of Cu^{2+} ions was up to 85% at pH 5.0. The adsorption equilibrium was reached within 30 min as initial solution concentration increased from 108 to

268 mg/L, and the process can be better described using the pseudo-second-order model than pseudo-first-order model. Isotherm data fitted well to the Langmuir isotherm model. The maximum adsorption capacity (q_m) calculated from Langmuir isotherm model of PAN-COOH nanofiber mats was 40.14 mg/g. Desorption results show that the adsorption capacity can remain up to 90% after five times usage.

Acknowledgment

The project is supported by the National Natural Science Foundation of China (5114304), the Opening Project of State Key Laboratory of Chemical Resource Engineering (CRE-2012-C-206) and the Central University of basic scientific research project of BUCT (ZZ1112).

Symbol list

C_0	—	initial concentration of Cu^{2+} in solution (mg/L)
C_e	—	the equilibrium concentration of Cu^{2+} (mg/L)
q_e	—	equilibrium adsorption capacity (mg/g)
m	—	mass of adsorbents (g)
V	—	volume of solution (L)
q_t	—	adsorption capacity at time t (mg/g)
K_1 and K_2	—	the pseudo-first-order and second-order rate constants
q_m	—	maximum adsorption capacity (mg/g)
b	—	langmuir constant related to the energy of adsorption (L/mg)
K_f and $1/n$	—	constants are related to the adsorption capacity and intensity of adsorption

References

[1] A.J. Miao, W.X. Wang, P. Juneau, Comparison of Cd, Cu, and Zn toxic effects on four marine phytoplankton by pulse-amplitude-modulated fluorometry, Environ. Toxicol. Chem. 24 (2005) 2603–2611.

[2] World Health Organization (WHO), Guidelines for Drinking-water Quality, 4th ed., WHO library Cataloguing-in-Publication Data, Geneva, 2011, pp. 340–341.

[3] H.C. Tao, M. Liang, W. Li, L.J. Zhang, J.R. Ni, W.M. Wu, Removal of copper from aqueous solution by electrodeposition in cathode chamber of microbial fuel cell, J. Hazard. Mater. 189 (2011) 186–192.

[4] F. Akbal, S. Camcı, Copper, chromium and nickel removal from metal plating wastewater by electrocoagulation, Desalination 269 (2011) 214–222.

[5] C. Nie, Y. Zhan, L. Pan, H. Li, Z. Sun, Electrosorption of different cations and anions with membrane capacitive deionization based on carbon nanotube/nanofiber electrodes and ion-exchange membranes, Desalin. Water Treat. 30 (2011) 266–271.

[6] A. Górka, J. Zamorska, D. Antos, Coupling ion exchange and biosorption for copper(II) removal from wastewaters, Ind. Eng. Chem. Res. 50 (2011) 3494–3502.

[7] Z.A. Alothman, Y.E. Unsal, M. Habila, M. Tuzen, M. Soylak, A membrane filtration procedure for the enrichment, separation, and flame atomic absorption spectrometric determinations of some metals in water, hair, urine, and fish samples, Desalin. Water Treat. doi:10.1080/19443994.2013.874958.

[8] W. Zhang, C. Cui, Z. Ren, Y. Dai, H. Meng, Simultaneous removal and recovery of copper(II) from acidic wastewater by hollow fiber renewal liquid membrane with LIX984N as carrier, Chem. Eng. J. 157 (2010) 230–237.

[9] C. Cojocaru, G. Zakrzewska-Trznadel, Response surface modeling and optimization of copper removal from aqua solutions using polymer assisted ultrafiltration, J. Membr. Sci. 298 (2007) 56–70.

[10] C. Liu, R. Bai, Adsorptive removal of copper ions with highly porous chitosan/cellulose acetate blend hollow fiber membranes, J. Membr. Sci. 284 (2006) 313–322.

[11] B. Medjahed, M.A. Didi, D. Villemin, Factorial design in optimization of extraction procedure for copper(II) using aliquat 336 and Tri-n-butylphosphate based supported liquid membrane, Desalin. Water Treat. doi:10.1080/19443994.2013.797626.

[12] W. Yantasee, Y. Lin, G.E. Fryxell, K.L. Alford, B.J. Busche, C.D. Johnson, Selective removal of copper(II) from aqueous solutions using fine-grained activated carbon functionalized with amine, Ind. Eng. Chem. Res. 43 (2004) 2759–2764.

[13] W. Chouyyok, Y. Shin, J. Davidson, W.D. Samuels, N.H. Lafemina, R.D. Rutledge, G.E. Fryxell, Selective removal of copper(II) from natural waters by nanoporous sorbents functionalized with chelating diamines, Environ. Sci. Technol. 44 (2010) 6390–6395.

[14] W. Maketon, C.Z. Zenner, K.L. Ogden, Removal efficiency and binding mechanisms of copper and copper-EDTA complexes using polyethyleneimine, Environ. Sci. Technol. 42 (2008) 2124–2129.

[15] A.A. Bsoul, L. Zeatoun, A. Abdelhay, M. Chiha, Adsorption of copper ions from water by different types of natural seed materials, Desalin. Water Treat. doi:10.1080/19443994.2013.808593.

[16] E. Pehlivan, T. Altun, Ş. Parlayici, Modified barley straw as a potential biosorbent for removal of copper ions from aqueous solution, Food Chem. 135 (2012) 2229–2234.

[17] S. Deng, R. Bai, J.P. Chen, Aminated polyacrylonitrile fibers for lead and copper removal, Langmuir 19 (2003) 5058–5064.

[18] S. Haider, S.Y. Park, Preparation of the electrospun chitosan nanofibers and their applications to the adsorption of Cu(II) and Pb(II) ions from an aqueous solution, J. Membr. Sci. 328 (2009) 90–96.

[19] X. Wang, M. Min, Z. Liu, Y. Yang, Z. Zhou, M. Zhu, Y. Chen, B.S. Hsiao, Poly(ethyleneimine) nanofibrous affinity membrane fabricated via one step wet-electrospinning from poly(vinyl alcohol)-doped poly (ethyleneimine) solution system and its application, J. Membr. Sci. 379 (2011) 191–199.

[20] M. Min, L. Shen, G. Hong, M. Zhu, Y. Zhang, X. Wang, Y. Chen, B.S. Hsiao, Micro-nano structure poly (ether sulfones)/poly(ethyleneimine) nanofibrous affinity membranes for adsorption of anionic dyes and heavy metal ions in aqueous solution, Chem. Eng. J. 197 (2012) 88–100.

[21] P. Kampalanonwat, P. Supaphol, Preparation and adsorption behavior of aminated electrospun polyacrylonitrile nanofiber mats for heavy metal ion removal, ACS Appl. Mater. Interfaces 2 (2010) 3619–3627.

[22] P.K. Neghlani, M. Rafizadeh, F.A. Taromi, Preparation of aminated-polyacrylonitrile nanofiber membranes for the adsorption of metal ions: comparison with microfibers, J. Hazard. Mater. 186 (2011) 182–189.

[23] P. Kampalanonwat, P. Supaphol, Preparation of hydrolyzed electrospun polyacrylonitrile fiber mats as chelating substrates: a case study on copper(II) ions, Ind. Eng. Chem. Res. 50 (2011) 11912–11921.

[24] X. Wang, Y. Zheng, A. Wang, Fast removal of copper ions from aqueous solution by chitosan-g-poly(acrylic acid)/attapulgite composites, J. Hazard. Mater. 168 (2009) 970–977.

[25] F. Liu, X. Luo, X. Lin, L. Liang, Y. Chen, Removal of copper and lead from aqueous solution by carboxylic acid functionalized deacetylated konjac glucomannan, J. Hazard. Mater. 171 (2009) 802–808.

[26] H. Yan, L. Yang, Z. Yang, H. Yang, A. Li, R. Cheng, Preparation of chitosan/poly(acrylic acid) magnetic composite microspheres and applications in the removal of copper(II) ions from aqueous solutions, J. Hazard. Mater. 229–230 (2012) 371–380.

[27] S.Y. Mak, D.H. Chen, Binding and sulfonation of poly (acrylic acid) on iron oxide nanoparticles: a novel, magnetic, strong acid cation nano-adsorbent, Macromol. Rapid Commun. 26 (2005) 1567–1571.

[28] J. Wang, K. Pan, Q. He, B. Cao, Polyacrylonitrile/polypyrrole core/shell nanofiber mat for the removal of hexavalent chromium from aqueous solution, J. Hazard. Mater. 244–245 (2013) 121–129.

[29] J. Wang, K. Pan, E.P. Giannelis, B. Cao, Polyacrylonitrile/polyaniline core/shell nanofiber mat for removal of hexavalent chromium from aqueous solution: mechanism and applications, RSC Adv. 3 (2013) 8978–8987.

[30] H. Lee, S.M. Dellatore, W.M. Miller, P.B. Messersmith, Mussel-inspired surface chemistry for multifunctional coatings, Science 318 (2007) 426–430.

[31] C. Li, W. Wang, F. Xu, L. Zhang, W. Yang, Preparation of pH-sensitive membranes via dopamine-initiated atom transfer radical polymerization, J. Membr. Sci. 367 (2011) 7–13.

[32] J.G. Speight, Lange's Handbook of Chemistry, 16th ed., McGraw-Hill, New York, NY, 2005, Section 3.14, p. 1255.

[33] E. Pehlivan, T. Altun, Ion-exchange of Pb^{2+}, Cu^{2+}, Zn^{2+}, Cd^{2+}, and Ni^{2+} ions from aqueous solution by Lewatit CNP 80, J. Hazard. Mater. 140 (2007) 299–307.

[34] N. Ferrah, O. Abderrahim, M.A. Didi, D. Villemin, Removal of copper ions from aqueous solutions by a new sorbent: Polyethyleneiminemethylene phosphonic acid, Desalination 269 (2011) 17–24.

[35] K. Pan, X. Zhang, J. Zhu, B. Cao, Grafting of regenerated cellulose membrane by surface-initiated atom transfer radical polymerization and its pH-resposive behavior, Polym. Adv. Technol. 22 (2011) 1948–1952.

[36] R.R. Krishni, K.Y. Foo, B.H. Hameed, Adsorption of cationic dye using a low-cost biowaste adsorbent: Equilibrium, kinetic, and thermodynamic study, Desalin. Water Treat. doi:10.1080/19443994.2013.815689.

[37] Y. Jiang, H. Pang, B. Liao, Removal of copper(II) ions from aqueous solution by modified bagasse, J. Hazard. Mater. 164 (2009) 1–9.

[38] K.Y. Shin, J.Y. Hong, J. Jang, Heavy metal ion adsorption behavior in nitrogen-doped magnetic carbon nanoparticles: Isotherms and kinetic study, J. Hazard. Mater. 190 (2011) 36–44.

[39] C.Y. Chen, C.L. Chiang, C.R. Chen, Removal of heavy metal ions by a chelating resin containing glycine as chelating groups, Sep. Purif. Technol. 54 (2007) 396–403.

[40] D.T. Sawyer, P.J. Paulsen, Properties and infrared spectra of ethylenediaminetetraacetic acid complexes. I. Alkaline Earth chelates, J. Am. Chem. Soc. 80 (1958) 1597–1600.

[41] D.T. Sawyer, P.J. Paulsen, Properties and infrared spectra of ethylenediaminetetraacetic acid Complexes. II. Chelates of divalent ions, J. Am. Chem. Soc. 81 (1958) 816–820.

[42] C.Y. Chen, C.Y. Chen, Stability constants of water-soluble and latex types of chelating polymers containing iminodiacetic acid with some transition-metal ions, Eur. Polym. J. 39 (2003) 991–1000.

[43] A.E. Martell, M. Calvin, Chemistry of the metal chelate compounds, 3rd ed., Prentice Hall, New York, NY, 1956, pp. 246–247.